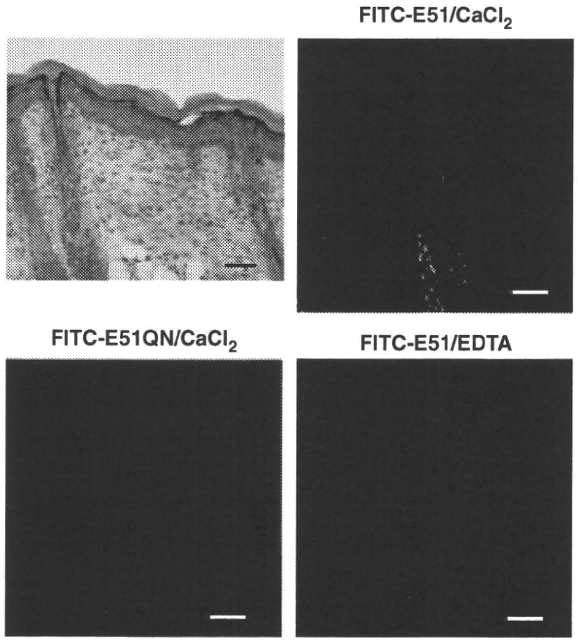

Fig. 6. Detection of *in situ* TGase 3 activities in the mouse skin section. Hematoxylin and eosin staining is shown at the left. FITC–pepE51 (1 μM) was reacted with frozen mouse skin section in the presence of $CaCl_2$. As a negative control, incubation with FITC–pepE51QN and co-presence of EDTA in the reaction of pepE51 were carried out under the same reaction condition. Bar represents 50 μm.

skin, as previously established for TGase 1-preferred substrate peptide, K5 [16]. Using a similar approach, calcium-dependent incorporation of FITC–pepE51 through its glutamine residue into lysine residues of endogenous substrate proteins was observed (Figs 6 and 7). TGase 3 has been observed in both differentiating keratinocytes and hair follicles of the epidermis by immunochemical analyses [38–40]. However, in this study, we present the first direct evidence for the detection of activated TGase 3 in the epidermis. Therefore, this finding provides more precise information on the physiological significance of TGase 3 because this enzyme is synthesized as an inactive zymogen form.

In the epidermis, endogenous TGase 3 activity was observed mostly in the granular and spinous layers. However, the activity was detected within a more limited region when compared with the staining results obtained with FITC–pepK5, a preferred substrate for TGase 1. In addition, in hair follicle cells, the staining pattern of TGase 3 was distinct from that of TGase 1. *In situ* activity of the enzyme was observed mainly around the inner root sheath, which is consistent with results obtained previously using immunostaining analyses [39,40]. By contrast, TGase 3 activity was found around the medulla and hair cortex. These results for TGase 3 in the epidermis and hair follicles are convincing; however, in cells with higher TGase 1 activity, there might be the possibility of a slight cross-reaction with TGase 1.

In a recent study that used immunochemical analysis and *in situ* detection of the activity by FITC-labeled cadaverine, Thibaut *et al.* [40] reported that TGase 3 was mainly present in hair fibers. This is mostly consistent with our results. However, in their study, the

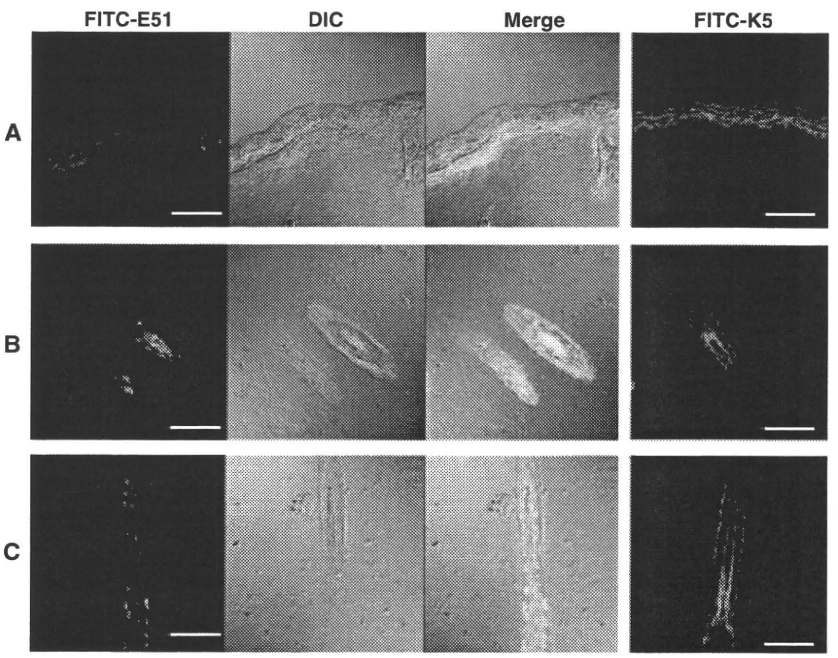

Fig. 7. *In situ* TGase activities detected with FITC-labeled peptides in the mouse skin epidermis and hair follicles. *In situ* activity of TGase 3 was detected under the observation at enlarged scale in the same reaction condition as described in the legend to Fig. 6. From left, FITC–pepE51 (1 μM), differential interference images and their merged images are aligned. FITC–pepK5 (1 μM) was paralleled in each experiment (right). (A) Skin epidermis, (B) transversal and (C) longitudinal sections of hair follicles. Bar represents 50 μm.

detection procedure for TGase *in situ* activity was not specific for TGase 3 in principle, because cadaverine is an amine substrate known to react with any active TGase.

Although aberrant TGase 1 activity has been reported in several skin diseases, as a consequence of genetic mutation [41,42], nothing has been reported regarding a TGase 3 defect in specific pathologies. Investigation of *in situ* activity of TGase 3 is a valuable method for elucidating the precise role of this isozyme in a variety of tissues and cells. Recently, detection of altered enzymatic activities in patients with TGase 1 mutation was successfully achieved using FITC–pepK5 [19]. Because this method is applicable for monitoring aberrant expression of TGase 3 activity, it will assist in the investigation unknown diseases which may be caused by TGase 3 mutations.

In conclusion, we have identified several preferred substrate sequences for TGase 3. The most reactive peptide sequence, E51, permitted the detection of *in vitro* and *in situ* activities of the active enzyme. In addition to pepK5, a specific preferred substrate peptide for TGase 1, pepE51 could become a useful tool to further characterize TGase activity and identify endogenous substrates in the skin and hair follicles.

Experimental procedures

Transglutaminases

For screening, human recombinant TGase 3 obtained by expression and purification from baculovirus-infected insect cells was used, as described previously [27]. For evaluation of the obtained sequences, recombinant human TGases 1, -2 and -3 and purified guinea-pig liver TGase were purchased from Zedira (Darmstadt, Germany) and Sigma (St. Louis, MO, USA). For the activation of TGase 3, the zymogen was proteolyzed by treatment with dispase (Roche, Mannheim, Germany). Human Factor XIII (Fibrogammin^{R}P; ZLB Behring, Marburg, Mannheim, Germany) was activated (Factor XIIIa) by treatment with bovine thrombin (Sigma).

Screening of preferred sequences from a phage-displayed peptide library

Screening was carried out as described previously, using an M13 PhD-12 phage-display system (New England Biolabs Inc., Ipswich, MA, USA) [15]. Briefly, $\sim 1.5 \times 10^{11}$ (first-round panning) phage clones were incubated at 37 °C with dispase-activated TGase 3 (1 ng·μL^{-1}) in 10 mM Tris/HCl (pH 8.0), 150 mM NaCl (TBS buffer) containing 1 mM dithiothreitol, 5 mM $CaCl_2$ and 5 mM bio-Cd [EZ-link™ 5-(biotinamido)pentylamine; Pierce Biotechnology, Rockford, IL, USA]. The catalytic reaction was stopped by the addition of EDTA. The phage particles were precipitated in the presence of poly-(ethylene glycol) and NaCl with salmon sperm DNA as a carrier. Next, phage clones that covalently incorporated bio-Cd were selected by affinity chromatography using mono-avidin gel (SoftLink™ Soft Release Avidin Resin; Promega Corp., Madison, WI, USA). After washing with TBS containing 0.1 or 0.5% Tween 20 and 2 mM EDTA and then with TBS, the bound phage particles were eluted by competition using 5 mM biotin in TBS buffer. The entire eluate was used to infect ER2738 host bacteria to amplify the phages. The phage particles were concentrated by precipitation with poly-(ethylene glygol)–NaCl and then used for subsequent rounds. After panning five times in all, DNA sequences of the displayed peptides of the selected phage clones were determined.

Construction of the expression vector for GST fusion proteins

The vector plasmid pET24d–GST(QN) was used to express modified GST, in which all the glutamine residues were substituted by asparagine residues, and fused with a peptide at the N-terminus and hexahistidine at the C-terminus [15]. The DNA of each phage was isolated and the sequences of the displayed 12-mer peptides were amplified by PCR. The amplified PCR products were digested and inserted into pET24d–GST(QN). To generate peptide mutants in which each amino acid was substituted to alanine, PCR-based mutagenesis was carried out.

Escherichia coli BL21(DE3)LysS or BL21(DE3)LysE was transformed with the plasmids and expression was induced by the addition of isopropyl β-D-thiogalactoside. Recombinant proteins were purified using TALON Metal Affinity Resin according to the manufacture's instructions (BD Bioscience, San Jose, CA, USA). The concentration of the purified protein was determined by quantification of the intensity for the separated bands in SDS/PAGE analysis using imaging software (MULTIGAUGE software; Fujifilm, Tokyo, Japan).

Evaluation of the preferred sequences using the recombinant proteins

The reactivities of recombinant GST(QN)-fusion proteins were evaluated by the incorporation of Dansyl-Cd (Sigma), a fluorescence-labeled pentylamine. Recombinant protein (200 ng·μL^{-1}) and 0.5 mM Dansyl-Cd were incubated in TBS containing 5 mM $CaCl_2$ and 1 mM dithiothreitol in the presence of activated TGase 3 (1 ng·μL^{-1}). Dimethylcasein (Sigma) was used as a positive control at a final concentration of 200 ng·μL^{-1}. The reaction mixture was incubated at 37 °C and then separated by 12.5% SDS/PAGE. A fluorograph of the gel was obtained by UV irradiation (254 nm) to visualize the amount of incorporated Dansyl-Cd. To quantify the results, the fluorescence intensity of each

product was analyzed using imaging software (MULTIGAUGE software).

Evaluation of synthetic peptides as a substrate

The 12-amino acid peptide corresponding to the E51 sequence (PPPYSFYQSRWV) was synthesized and biotinylated at the N-terminus (pepE51). A mutant peptide in which glutamine was substituted to asparagine was also synthesized (PPPYSFYNSRWV) and biotinylated as pepE51QN. TGase 1-, TGase 2- and Factor XIII-preferred substrate biotinylated peptides, being pepK5 (YEQHKLPSSWPF), pepT26 (HQSYVDPWMLDH) and pepF11 (DQMMLPWPAVAL), respectively, were used for comparison.

To evaluate the activity and specificity of the peptides, a microtiter plate assay was performed as described previously [32,33]. Spermine, as a primary amine, was immobilized covalently onto microplates. The enzyme reaction mixture, in a total volume of 100 μL, contained biotinylated peptide in the presence of the enzymes in an appropriate buffer (final concentration: 20 mM Tris/HCl, pH 8.3, 140 mM NaCl, 2.5 mM dithiothreitol, 15 mM $CaCl_2$). The microtiter plates were incubated at 37 °C for the indicated time intervals and the reaction was stopped by the addition of EDTA (50 mM at final concentration). The wells were then washed with a Tris-based buffer (10 mM Tris/HCl, pH 8.0, 150 mM NaCl, 0.1% Tween-20). The incorporated biotinylated peptides were detected using streptavidin-peroxidase (Rockland Immunochemicals Inc., Gilbertsville, PA, USA) and the peroxidase substrate 3,3′,5,5′-tetramethylbenzidine (Sigma).

Detection of *in situ* TGase activities in the mouse skin sections

Animal care and experiments were conducted according to the Regulations for Animal Experiments in Nagoya University.

Immediately after the mice had been killed by diethylether anesthetization, the skin was dissected and embedded in medium (Sakura Finetek, Tokyo, Japan) as a standard method. Frozen sections were dissected into 4–8 μm slices and kept frozen until use. Fluorescence-labeled peptides (FITC–pepE51, FITC–pepE51QN and FITC–pepK5) were synthesized.

For the reaction, sections were dried and then blocked by incubation in NaCl/P_i containing 1% BSA (Sigma) for 30 min at room temperature. Sections were incubated for 90 min with a solution containing 100 mM Tris/HCl (pH 8.0), 5 mM $CaCl_2$ or 5 mM EDTA and 1 mM dithiothreitol, in the presence of FITC-labeled peptide at 37 °C. After washing with NaCl/P_i three times, anti-fading solution was mounted onto the section with a cover-glass. Differential interference images and fluorescence were analyzed with a confocal laser-scanning microscope, LSM5 PASCAL (Zeiss, Göttingen, Germany). For hematoxylin and eosin staining, the tissue section was fixed, then stained using standard methods and analyzed with a microscope, BZ-8100 (Keyence, Osaka, Japan).

Acknowledgements

We greatly appreciate Dr Masatoshi Maki and Dr Hideki Shibata in our laboratory for providing valuable suggestions. This work was supported by a Grant-in-Aid for Scientific Research on Innovative Areas (No. 20200072) from the Ministry of Education, Sports, Science and Technology (MEXT, Japan) (to KH) and the Marie Curie Action RTN program 'Transglutaminase: role in pathogenesis, diagnosis and therapy' (TRACKS; contract No. MRTN-CT-2008-36032).

References

1 Griffin M, Casadio R & Bergamini CM (2002) Transglutaminases: nature's biological glues. *Biochem J* **368**, 377–396.
2 Lorand L & Graham RM (2003) Transglutaminases: crosslinking enzymes with pleiotropic functions. *Nat Rev Mol Cell Biol* **4**, 140–156.
3 Ichinose A (2001) Physiopathology and regulation of Factor XIII. *Thromb Haemost* **86**, 57–65.
4 Fésüs L & Piacentini M (2002) Transglutaminase 2: an enigmatic enzyme with diverstic functions. *Trends Biochem Sci* **27**, 534–539.
5 Fésüs L & Szondy Z (2005) Transglutaminase 2 in the balance of cell death and survival. *FEBS Lett* **579**, 3297–3302.
6 Telci D & Griffin M (2006) Tissue transglutaminase (TG2) – a wound response enzyme. *Front Biosci* **11**, 867–882.
7 Eckert RL, Sturniolo MT, Broome AM, Ruse M & Rorke EA (2005) Transglutaminase function in epidermis. *J Invest Dermatol* **124**, 481–492.
8 Hitomi K (2005) Transglutaminase in skin epidermis. *Eur J Dermatol* **15**, 313–319.
9 Zeeuwen PL (2004) Epidermal differentiation: the role of proteases and their inhibitors. *Eur J Cell Biol* **83**, 761–773.
10 Esposito C, Pucci P, Amoresano A, Marino G, Cozzolino A & Porta R (1996) Transglutaminase from rat coagulating gland secretion. Post-translational modification and activation by phosphatidic acids. *J Biol Chem* **271**, 27416–27423.
11 Candi E, Oddi S, Paradisi A, Terrinoni A, Ranalli M, Teofoli P, Citro G, Scarpato S, Puddu P & Melino G (2002) Expression of transglutaminase 5 in normal and pathologic human epidermis. *J Invest Dermatol* **119**, 670–677.

12 Pietroni V, Di Giorgi S, Paradisi A, Ahvazi B, Candi E & Melino G (2008) Inactive and highly active, proteolytically processed transglutaminase-5 in epithelial cells. *J Invest Dermatol* **128**, 2760–2766.
13 Esposito C & Caputo I (2005) Mammalian transglutaminases: identification of substrates as a key to physiological function and physiological relevance. *FEBS J* **272**, 615–631.
14 Facchiano A & Facchiano F (2009) Transglutaminases and their substrates in biology and human diseases: 50 years of growing. *Amino Acids* **36**, 599–614.
15 Sugimura Y, Hosono M, Wada F, Yoshimura T, Maki M & Hitomi K (2006) Screening for the preferred substrate sequence of transglutaminase using a phage-displayed peptide library: identification of peptide substrates for TGase 2 and Factor XIIIa. *J Biol Chem* **281**, 17699–17706.
16 Sugimura Y, Hosono M, Kitamura M, Tsuda T, Yamanishi K, Maki M & Hitomi K (2008) Identification of preferred substrate sequences for transglutaminase 1-development of a novel peptide that can efficiently detect cross-linking enzyme activity in the skin. *FEBS J* **275**, 5667–5677.
17 Sugimura Y, Yokoyma K, Nio N, Maki M & Hitomi K (2008) Identification of preferred substrate sequences of microbial transglutaminase from Streptomyces mobaraensis using a phage-displayed peptide library. *Arch Biochem Biophys* **477**, 379–383.
18 Hitomi K, Kitamura M & Sugimura Y (2009) Preferred substrate sequences for transglutaminase 2: screening using a phage-displayed peptide library. *Amino Acids* **36**, 619–624.
19 Akiyama M, Sakai K, Yanagi T, Fukushima S, Ihn H, Hitomi K & Shimizu H (2010) Transglutaminase 1 preferred substrate peptide K5 is an efficient tool in diagnosis of lamellar ichthyosis. *Am J Pathol* **176**, 1592–1599.
20 Sugimura Y, Ueda H, Maki M & Hitomi K (2007) Novel site-specific immobilization of a functional protein using a preferred substrate sequence for transglutaminase 2. *J Biotechnol* **131**, 121–127.
21 Kim HC, Lewis MS, Gorman JJ, Park SC, Girard JE, Folk JE & Chung SI (1990) Protransglutaminase E from guinea pig skin. Isolation and partial characterization. *J Biol Chem* **265**, 21971–21978.
22 Kim I-G, Gorman JJ, Park S-C, Chung S-I & Steinert PM (1993) The deduced sequence of the novel protransglutaminase E (TGase3) of human and mouse skin. *J Biol Chem* **268**, 12682–12690.
23 Kalinin AE, Kajava AV & Steinert PM (2002) Epithelial barrier function: assembly and structural features of the cornified envelop. *Bioessays* **24**, 789–800.
24 Candi E, Schmidt R & Melino G (2005) The cornified envelope: a model of cell death in the skin. *Nat Rev Mol Cell Biol* **6**, 328–340.
25 Cheng T, Hitomi K, van Vlijmen-Willems IM, Jongh G, Yamamoto K, Nishi K, Watts C, Reinheckel T, Schalkwijk J & Zeeuwen PM (2006) Cystatin M/E is a high affinity inhibitor of cathepsin V and the short chain form of cathepsin L by a reactive site that is distinct from the legumain-binding site. A novel clue for the role of cystatin M/E in epidermal cornification. *J Biol Chem* **281**, 15893–15899.
26 Zeeuwen PM, Cheng T & Schalkwijk J (2009) The biology of cystatin M/E and its cognate target protease. *J Invest Dermatol* **129**, 1327–1338.
27 Hitomi K, Kanehiro S, Ikura K & Maki M (1999) Characterization of recombinant mouse epidermal-type transglutaminase (TGase 3): regulation of its activity by proteolysis and guanine nucleotides. *J Biochem (Tokyo)* **125**, 1048–1054.
28 Hitomi K, Horio Y, Ikura K, Yamanishi K & Maki M (2001) Analysis of epidermal-type transglutaminase expression in mouse tissues and cell lines. *Int J Biochem Cell Biol* **33**, 491–498.
29 Ahvazi B, Boeshans KM, Idler W, Baxa U & Steinert P (2003) Roles of calcium ions in the activation and activity of the transglutaminase 3 enzyme. *J Biol Chem* **278**, 23834–23841.
30 Hitomi K, Presland RB, Nakayama T, Fleckman P, Dale BA & Maki M (2003) Analysis of epidermal-type transglutaminase (transglutaminase 3) in human stratified epithelia and cultured keratinocytes using monoclonal antibodies. *J Dermatol Sci* **32**, 95–103.
31 Ahvazi B, Boeshans KM & Rastinejad F (2004) The emerging structural understanding of transglutaminase 3. *J Struct Biol* **147**, 200–207.
32 Alea MP, Kitamura M, Martin G, Thomas V, Hitomi K & El Alaoui S (2009) Development of a highly sensitive and specific colorimetric assay for the measurement of TGase 2 cross-linking activity. *Anal Biochem* **389**, 150–156.
33 Hitomi K, Kitamura M, Alea MP, Ceylan I, Thomas V & El Alaoui S (2009) A specific colorimetric assay for measuring of transglutaminase 1 and Factor XIII activities. *Anal Biochem* **394**, 281–283.
34 Brown DR, Kitchin D, Qadadri B, Neptune N, Batteiger T & Ermel A (2006) The human papillomavirus type 11 E1^E4 protein is a transglutaminase 3 substrate and induces abnormalities of the cornified cell envelope. *Virology* **345**, 290–298.
35 Tarcsa E, Candi E, Kartasova T, Idler WW, Marekov LN & Steinert PM (1998) Structural and transglutaminase substrate properties of the small proline-rich 2 family of cornified cell envelope proteins. *J Biol Chem* **273**, 23297–23303.
36 Candi E, Tarcsa E, Idler WW, Kartasova T, Marekov LN & Steinert PM (1999) Transglutaminase cross-linking properties of the small proline-rich 1 family of

cornified cell envelope proteins. Integration with loricrin. *J Biol Chem* **274**, 7226–7237.
37 Candi E, Melino G, Mei G, Tarcsa E, Chung S-I, Marekov LN & Steinert PM (1995) Biochemical, structural, and transglutaminase substrate properties of human loricrin, the major epidermal cornified cell envelope protein. *J Biol Chem* **270**, 26382–26390.
38 Tarcsa E, Marekov LN, Andreoli J, Idler WW, Candi E, Chung S-I & Steinert P (1997) The fate of trichohyalin: sequential post-translational modifications by peptidyl-arginine deiminase and transglutaminase. *J Biol Chem* **272**, 27893–27901.
39 Akiyama M, Matsuo I & Shimizu H (2002) Formation of cornified cell envelope in human hair follicle development. *Br J Dermatol* **146**, 968–976.
40 Thibaut S, Cavusoglu N, Becker E, Zerbib F, Bednarczk A, Schaeffer C, Dorsselaer A & Bernard B (2009) Transglutaminase-3 enzyme: a putative actor in human hair shaft scaffolding? *J Invest Dermatol* **129**, 449–459.
41 Huber M, Rettler I, Bernasconi K, Frenk E, Lavrijsen SPM, Ponec M, Bon A, Lautenschlager S, Schorderet DF & Hohl D (1995) Mutations of keratinocyte transglutaminase in lamellar ichthyosis. *Science* **267**, 525–528.
42 Akiyama M, Takizawa Y, Suzuki Y, Ishiko A, Matsuo I & Shimizu H (2001) Compound heterozygous TGM1 mutations including a novel missense mutation L204Q in a mild form of lamellar ichthyosis. *J Invest Dermatol* **116**, 992–995.

Supporting information

The following supplementary material is available:
Fig. S1. Screening procedure for substrate sequences preferred by TGase 3 using a phage-displayed random peptide library.

This supplementary material can be found in the online version of this article.

Please note: As a service to our authors and readers, this journal provides supporting information supplied by the authors. Such materials are peer-reviewed and may be re-organized for online delivery, but are not copy-edited or typeset. Technical support issues arising from supporting information (other than missing files) should be addressed to the authors.

H. Silm
Clinic of Dermatology, University of Tartu, Estonia

S. Kõks[a,b,c,*]
[a]*Department of Physiology, University of Tartu, Estonia*
[b]*Centre of Translational Medicine, University of Tartu, Estonia*
[c]*Institute of Veterinary Medicine and Animal Sciences, Estonian University of Life Sciences, Estonia*

*Corresponding author at: Department of Physiology, University of Tartu, 19 Ravila Street, 50411 Tartu, Estonia. Tel.: +372 7 374 335; fax: +372 7 374 332
E-mail address: Sulev.Koks@ut.ee (S. Kõks)

27 April 2010

doi:10.1016/j.jdermsci.2010.08.004

Letter to the Editor

ABCA12 dysfunction causes a disorder in glucosylceramide accumulation during keratinocyte differentiation

Harlequin ichthyosis (HI) is an autosomal recessive congenital ichthyoses, and patients of this disease frequently present with severe hyperkeratosis and scales over all of their epidermal surfaces. Recently, the gene encoding ABCA12 was identified as a causative gene for HI [1]. Since dysfunction in ABCA12 causes a decrease in epidermal ceramide (Cer) content concomitantly with loss of the skin lipid barrier, ABCA12 is thought to regulate epidermal generation of Cer. However, so far no direct target of ABCA12 has been identified. Thus, we attempted to study the substrate of ABCA12 by generating an ABCA12-deficient keratinocyte cell line and then comparing its sphingolipid metabolism to that of a normal keratinocyte cell line. Keratinocytes were isolated from a HI patient and a healthy donor [1], then were immortalized by expressing the T-antigen of SV40. After 15 passages, the morphology of the cells became uniform and we confirmed the expression of the SV40 T-antigen by Western blotting (Fig. 1A and B). The cell lines thus generated from the cells isolated from the HI patient and healthy donors were named HIKT and KT1, respectively. Genomic analysis revealed one mutation in the HIKT cells, from A to G adjacent a splice acceptor site of exon 24 (Fig. 1C). This mutation produced two splice variants of 674-bp and 513-pb (Fig. 1D). The 674-bp results from 9-bp lost from exon 24, and the 513-bp results from 170-bp lost from exon 24. This mutation has been reported to seriously affect the function of the ABCA12-protein [1]. We have successfully established an ABCA12-impaired keratinocyte cell line.

Several groups have demonstrated that the expression level of ABCA12 increases during the differentiation of keratinocytes, so that anaplastic keratinocytes express only low levels of ABCA12 [2,3]. As shown in Fig. 2A, anaplastic KT1 scarcely expresses any ABCA12. So, we attempted to induce differentiation of KT1 and HIKT cells, and thereby express high levels of ABCA12 in the cells. We induced differentiation in KT1 and HIKT cells and confirmed the differentiation by measuring the differentiation marker involcurin, which increased significantly in both cell lines during differentiation (3.1-fold increase in KT1 and 2.4-fold increase in HIKT) (Fig. 2A). We further found that ABCA12 also increased during differentiation, with especially high levels of expression at 7 days after induction in the HIKT cells. Following the induction of differentiation in KT1 and HIKT cells, their sphingolipid metabolism was examined at 7 days by labeling the cells with [^{3}H]dihydosphingosine or [^{14}C]galactose (Fig. 2B and C, respectively). Interestingly, apparent accumulations of [^{3}H]GlcCer (Fig. 2B) and [^{14}C]GlcCer (Fig. 2C) were observed in KT1 cells at 7 days post-induction compared to HIKT cells (203% increase at [^{3}H]GlcCer and 181% increase at [^{14}C]GlcCer, respectively). It is noteworthy that [^{14}C]gangliosides levels in KT1 cells were lower rather than equal to levels in HIKT cells (31% reduction), despite the accumulation of GlcCer. Since the ABCA12 is known to localize at lamellar bodies (LBs) in keratinocyte [4], this result indicates that differentiated KT1 cells aggressively accumulate GlcCer in LBs and not in the Golgi apparatus. Our results clearly demonstrate that ABCA12 deficiency impairs the GlcCer accumulation in LBs, thereby strongly indicating that ABCA12 transports GlcCer to the inner leaflet of LBs (Fig. 2D). Mass spectrometer analysis of accumulated

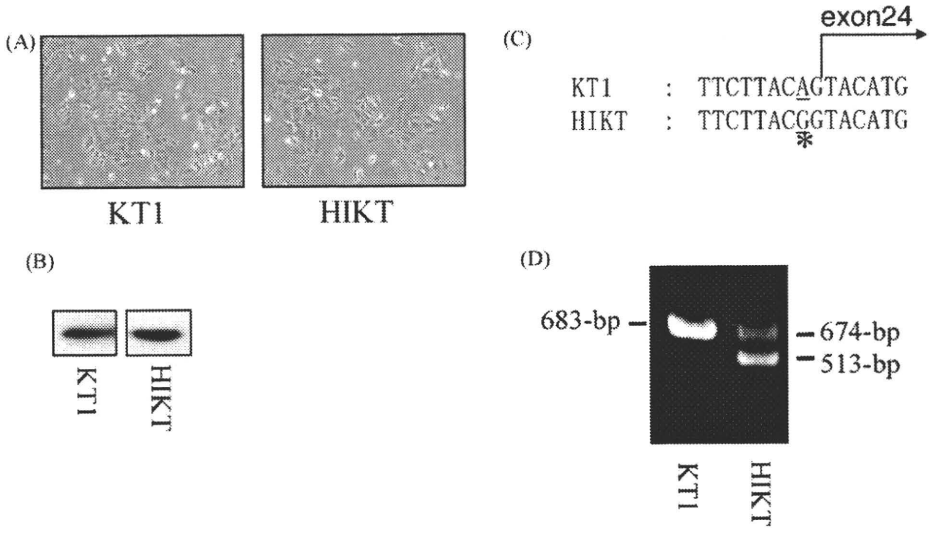

Fig. 1. KT1 and HIKT keratinocyte cell lines. KT1 and HIKT keratinocyte cell lines were generated by introducing the SV40 T-antigen into the cells using the culture supernatant of ΨCRIP-pMFGtsT (distributed from RIKEN cell bank, Tsukuba, Japan). After 15 passages, KT1 and HIKT cells exhibited similar morphology (A), and expected expression levels of T-antigen as examined by Western blotting using anti-SV40 LT (BD biosciences, NJ) (B). Genomic structures of KT1 and HIKT cells neighboring exon 24 (C). *A mutation from A to G in HIKT cells. RT-PCR analysis of mRNA fragments around the exon 23–24 boundary was performed as described previously [1] (D).

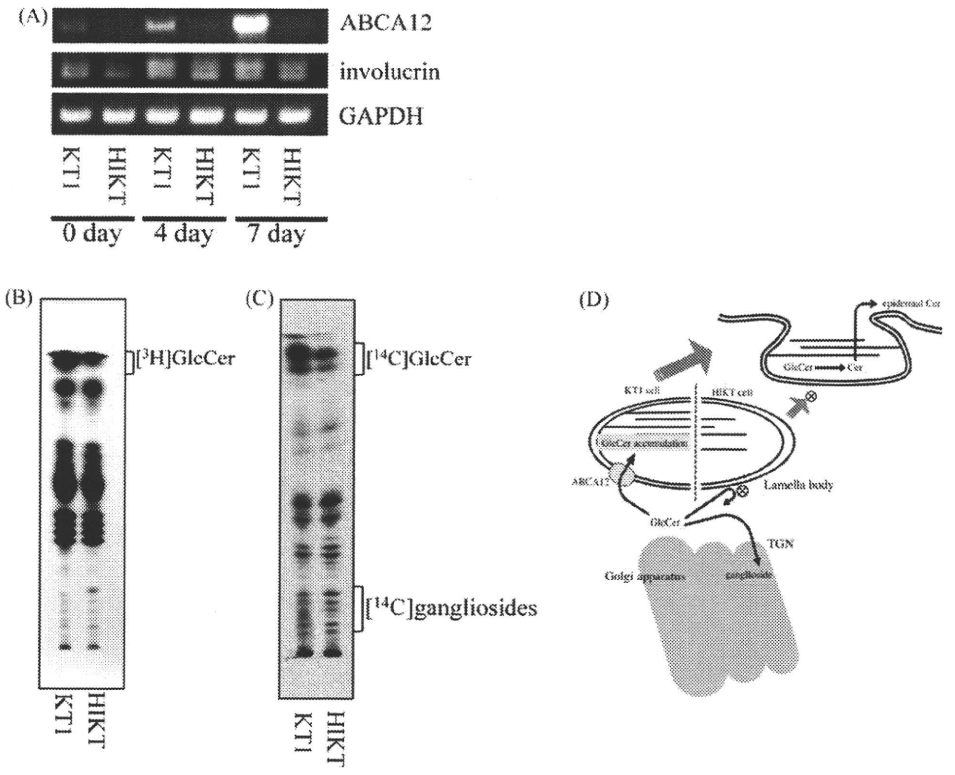

Fig. 2. Sphingolipids in KT1 and HIKT 4 days after induction of differentiation. (A) To induce differentiation, HIKT and KT1 cells were cultured in a DMEM/F-12 (2:1) mixture containing 10% fetal bovine serum, 1.2 mM Ca^{2+}, 10 μg/ml insulin, and 0.4 μg/ml ascorbic acid (differentiation medium) at 39 °C. Before (0 day) and 4 days and 7 days after induction, total RNA was isolated from each cell line, and semi-quantitative RT-PCR was performed using primers for ABCA12, 5′-GAATTGCAAACTGGAAGGAACTCCC-3′ and 5′-GAGTCAGCTAGGATTAGACAGC-3′; for involcurin, 5′-CTCCTCAAGACTGTTCCTCC-3′ and 5′-GCAGTCATGTGCTTTTCCTCTTGC-3′; for GAPDH, 5′-ATCACTGCCACCCAGAAGAC TGTGGA-3′ and 5′-GAGCTTGACAAAGTTGTCATTGAGAGC-3′. Seven days after induction of differentiation, HIKT and KT1 cells (10^6) were metabolically labeled with [^{3}H]dihydrosphingosine (2 μCi) (B) or [^{14}C]galactose (5 μCi) (C), then lipids were extracted and applied to HPTLC plates as described previously [5]. The HPTLC plates were developed with chloroform/methanol/0.05% $CaCl_2$ (60:35:8). The data are representative of tree independent experiments. (D) A possible mechanism of how to generate epidermal ceramides.

GlcCer will provide advanced information about substance preference of ABCA12. This remains for future study.

References

[1] Akiyama M, Sugiyama-Nakagiri Y, Sakai K, McMillan JR, Goto M, Arita K, et al. Mutations in lipid transporter ABCA12 in harlequin ichthyosis and functional recovery by corrective gene transfer. J Clin Invest 2005;115:1777–84.
[2] Jiang YJ, Lu B, Kim P, Paragh G, Schmitz G, Elias PM, et al. PPAR and LXR activators regulate ABCA12 expression in human keratinocytes. J Invest Dermatol 2008;128:104–9.
[3] Jiang YJ, Uchida Y, Lu B, Kim P, Mao C, Akiyama M, et al. Ceramide stimulates ABCA12 expression via peroxisome proliferator-activated receptor {delta} in human keratinocytes. J Biol Chem 2009;284:18942–5.
[4] Yamanaka Y, Akiyama M, Sugiyama-Nakagiri Y, Sakai K, Goto M, McMillan JR, et al. Expression of the keratinocyte lipid transporter ABCA12 in developing and reconstituted human epidermis. Am J Pathol 2007;171:43–52.
[5] Takeda S, Mitsutake S, Tsuji K, Igarashi Y. Apoptosis occurs via the ceramide recycling pathway in human HaCaT keratinocytes. J Biochem 2006;139:255–62.

Susumu Mitsutake[1]
Department of Biomembrane and Biofunctional Chemistry, Faculty of Advanced Life Sciences, Hokkaido University, Nishi 11, Kita 21, Kita-ku, Sapporo 001-0021, Japan

Chihiro Suzuki[1]
Department of Biomembrane and Biofunctional Chemistry, Faculty of Advanced Life Sciences, Hokkaido University, Nishi 11, Kita 21, Kita-ku, Sapporo 001-0021, Japan

Masashi Akiyama
Department of Dermatology, Hokkaido University Graduate School of Medicine, Nishi 7, Kita 15, Kita-ku, Sapporo 060-8638, Japan

Kiyomi Tsuji
Department of Biomembrane and Biofunctional Chemistry, Faculty of Advanced Life Sciences, Hokkaido University, Nishi 11, Kita 21, Kita-ku, Sapporo 001-0021, Japan

Teruki Yanagi, Hiroshi Shimizu
Department of Dermatology, Hokkaido University Graduate School of Medicine, Nishi 7, Kita 15, Kita-ku, Sapporo 060-8638, Japan

Yasuyuki Igarashi*
Department of Biomembrane and Biofunctional Chemistry, Faculty of Advanced Life Sciences, Hokkaido University, Nishi 11, Kita 21, Kita-ku, Sapporo 001-0021, Japan

*Corresponding author at: Hokkaido University, Department of Biomembrane and Biofunctional Chemistry, Graduate School of Pharmaceutical Sciences, Nishi 11, Kita 21, Kita-ku, Sapporo 001-0021, Japan.
Tel.: +81 11 706 9086; fax: +81 11 706 9047
E-mail address: yigarash@pharm.hokudai.ac.jp (Y. Igarashi)

[1]These authors contributed equally to this work.

8 April 2010

doi:10.1016/j.jdermsci.2010.08.012

THE JOURNAL OF DERMATOLOGY

doi: 10.1111/j.1346-8138.2009.00759.x

Journal of Dermatology 2010; **37**: 276–279

LETTER TO THE EDITOR

Linear immunoglobulin A bullous dermatosis associated with herpes simplex virus infection and Kawasaki disease

Dear Editor,

Linear immunoglobulin (Ig)A bullous dermatosis (LAD) is an autoimmune subepidermal bullous disease that involves IgA anti-basement membrane antibody and was suggested as an entity by Chorzelski and colleagues in 1979.[1] Its clinical characteristics are vesicles distributed annularly around erythema and/or sparsely distributed tense bullae. Direct immunofluorescence (DIF) shows linear deposition of IgA at the basement membrane zone. The pathogenesis of LAD remains unknown. LAD may occur following varicella zoster virus infection, may accompany malignancy and may be drug induced.[2,3] Kawasaki disease (KD) is an acute febrile eruptive disease that was described in 1967 by Kawasaki and preferentially affects younger children.[4] It is characterized by various kinds of skin rash and systemic vasculitis. The pathogenesis of this disease has been suggested to be a viral infection, such as Epstein–Barr virus or herpes simplex virus (HSV), toxic shock syndrome toxin-1 (TSST-1) and endotoxin from Gram-negative cocci; however, it remains unknown.[5] HSV infection could be causative for both KD and LAD, but their coexistence has not been reported. Recently, Rowley and coworkers[6,7] reported that IgA plasma cell infiltration is observed at the involved vascular wall in KD patients, and such infiltrates are also seen in unaffected regions, such as the upper respiratory tract, pancreas and kidney. These are interesting findings when considering the coexistence of LAD and KD.

A 14-month-old boy was admitted to our division for pruritic erythematous plaques and blisters scattered across his body. His past medical history was not remarkable and neither did he have a history of atopic dermatitis, chickenpox and HSV infection. At first, he presented to the Division of Pediatrics due to fever of unknown origin, and he was admitted the next day. When cervical lymphadenopathy, reddening of the lips, skin rash, conjunctivitis and indurative edema of extremities appeared, he was diagnosed with KD 3 days after the onset of symptoms. i.v. immunoglobulin (IVIG) and urinastatin were administrated, and his condition including skin rash gradually improved. Acetylsalicylic acid was also administrated after 11 days to prevent cardiovascular complications. After 16 days, pruritic erythematous plaques and blisters appeared in the inguinal area, scrotum, perineum, face and neck (Fig. 1). Mucosal involvement was not seen. Blister was tense and large bullae without delle. Viral infection or autoimmune blister disease was suspected, and viral investigation was carried out. Blister fluid from a trunk blister was collected aseptically by inserting a sterile needle into the blister and aspirating the fluid. Spinal fluid was collected by a conventional technique. HSV DNA was detected in the spinal fluid taken after 9 and 20 days and also in the blister fluid after 20 days with the method described by Aurelius and colleagues.[8] The serum HSV IgG titer was elevated (Table 1). There was no suggestive symptom of herpetic meningitis. Administration of i.v. acyclovir was not effective. The patient was referred to our division for further examination and treatment.

Blood tests showed increased white blood cell count (20 980/μL) and C-reactive protein of 0.52 mg/dL (normal <0.24). Liver function, renal function and serum Ig were all within normal limits. Biopsy from a blister on his back showed subepidermal blister formation and mild inflammatory infiltration that consisted of lymphocytes, neutrophils and partially of eosinophils in the upper dermis (Fig. 2). An

Correspondence: Masahiro Hayashi, Ph.D., Division of Dermatology, Yamagata Prefectural Shinjo Hospital, Wakaba-Cho 12-55, Shinjo 996-0025, Japan. Email: czk11223@nifty.ne.jp

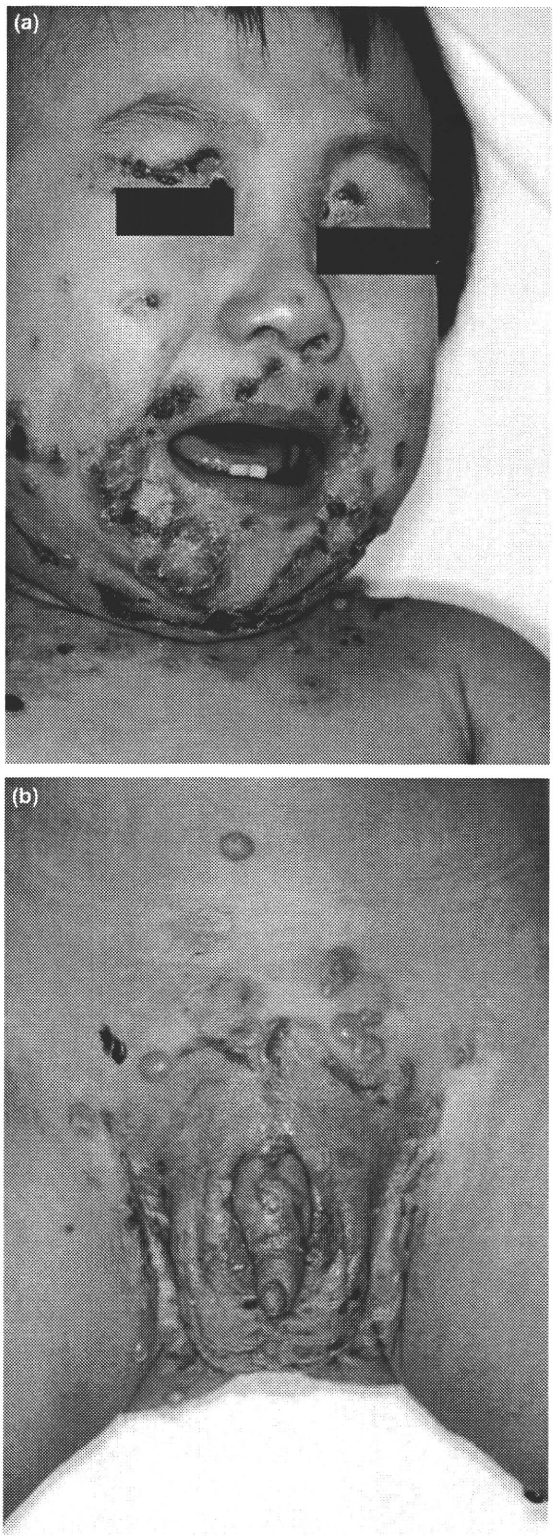

Figure 1. Pruritic erythematous plaques and blisters are seen on the (a) face, neck, (b) inguinal area, scrotum, and perineum.

Table 1. Serum viral titer

Days after KD onset	0	7	20
HSV IgM (<0.80)	0.21	0.16	0.31
HSV IgG (<2.0)	<2.0	≥**128.0**	**55**

Blister appeared 16 days after onset. The virus titer that comes off from the reference range is indicated by the bold. HSV, herpes simplex virus; Ig, immunoglobulin; KD, Kawasaki disease.

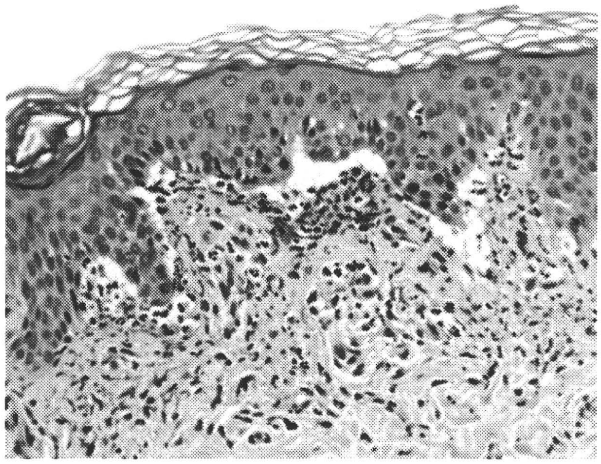

Figure 2. Subepidermal blister formation and mild inflammatory infiltration consisting of lymphocytes and partially of eosinophils in the upper dermis (hematoxylin–eosin stain, original magnification ×200).

intraepidermal neutrophilic microabscess was also observed. Vasculitis, balloon cell or intranuclear inclusion body were not seen. Tzanck test was not performed. DIF revealed linear deposition of IgA at the basement membrane zone (Fig. 3a). Indirect immunofluorescence of 1 mol/L NaCl-split human skin demonstrated that the epidermal side was positive for IgA antibodies at a titer of 1/40 (Fig. 3b). Immunoblotting studies identified that the patient's serum reacted with the 120-kDa antigen (linear IgA bullous dermatosis antigen, LAD-1) (Fig. 4). Finally we diagnosed this case as LAD, lamina lucida type. Acetylsalicylic acid was discontinued due to suspected drug-induced LAD; however, the symptoms did not improve. Oral prednisolone (PSL) 10 mg/day and 4,4-diaminodiphenyl-sulfone (DDS) 10 mg/day were administrated, and blisters and erosions rapidly epithelialized. Then, both were gradually tapered, PSL to 2.5 mg/day and DDS to 2.5 mg/day, and the boy showed persistent high grade fever for more than 5 days,

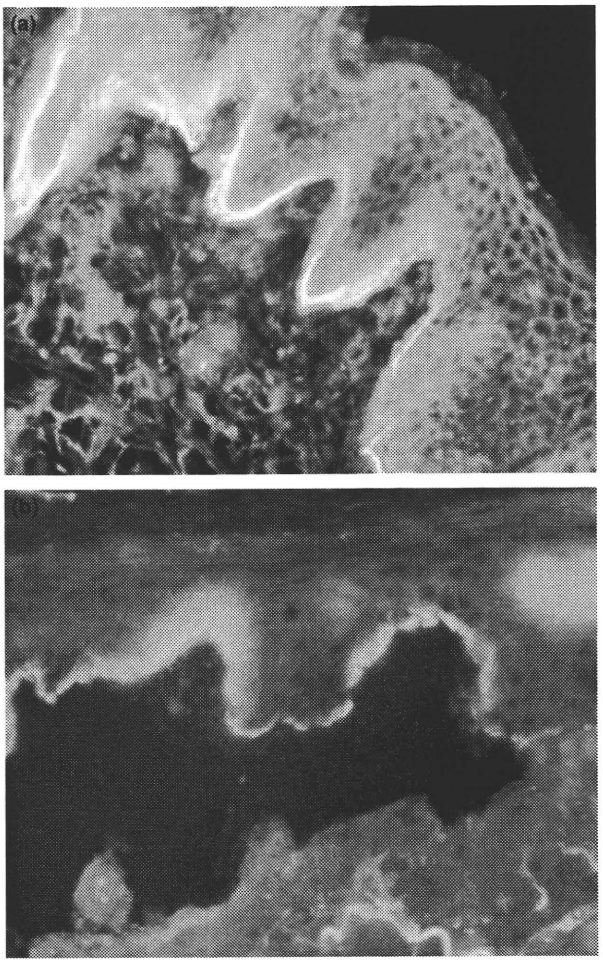

Figure 3. Direct immunofluorescence revealed linear deposition of immunoglobulin (Ig)A at the basement membrane zone (a). Indirect immunofluorescence on 1 mol/L NaCl-split human skin demonstrated that IgA antibodies were positive for the epidermal side at a titer of 1/40 (b).

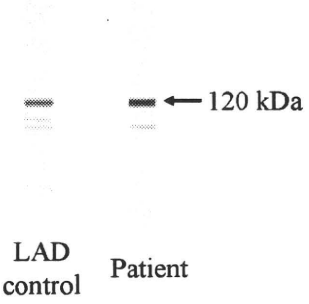

Figure 4. Immunoblotting studies identified that the patient's serum reacted with the 120-kDa antigen. LAD, linear immunoglobulin A bullous dermatosis.

cervical lymphadenopathy, reddening of the lips and tongue, skin rash and conjunctivitis. He was diagnosed as KD again. PSL and DDS were discontinued immediately. IVIG was effective for KD as well as at first onset. Acetylsalicylic acid was also administrated again and resurgence of LAD was not seen. To date, 32 months after KD settled, the patient has been well, and there have been no additional symptoms of KD and LAD.

The trigger of LAD is unknown. Post-chicken pox and drug-induced LAD have been reported.[2] In our case, HSV DNA was detected in both the spinal fluid and the blister fluid, and the HSV IgG titer was elevated, suggesting systemic HSV infection. Blister was clinically considered due to LAD but not HSV because they were tense and large bullae without delle. In addition, we could not find the unique histological features of herpes simplex from skin biopsy, hence there is a possibility that detection of HSV DNA from the blister fluid may have been by contamination of systemic infection of HSV. Although serum HSV IgG titer may also have been influenced by the administration of IVIG, we considered that HSV infection actually existed because HSV DNA was detected from spinal fluid. To our knowledge, this is the first case of LAD following HSV infection. Acetaminophen-induced LAD has been reported.[3] We ruled out this case from drug-induced LAD, because urinastatin was discontinued before the onset of LAD and symptoms did not recur when IVIG and acetylsalicylic acid were reinstituted.

Kawasaki disease involves systemic vasculitis, especially in the coronary arteries, resulting in aneurysm formation that is often fatal.[4] Although multiple infectious agents and toxins including HSV have been considered as the implication of the etiology of KD and many studies were investigated, none have been identified so far.[5] Various kinds of skin rash (so-called undefined skin rash) may be observed in patients with KD, even pustule and chicken pox-like eruptions.[9,10] LAD-like eruptions in KD have not been described so far. Recently, IgA plasma cell infiltration has been observed at the vascular wall,[6] and also in the upper respiratory tract, pancreas and kidney.[7] These findings suggest that an IgA immune response may spread to various organs, even in patients without vasculitis, by entry of the etiological agent through the upper respiratory tract.[7,11,12] Other investigators

have reported that patients with KD show increasing serum levels of IgA class antibodies to several antigens.[13,14] In our case, there is the possibility that antecedent KD and HSV infection may have triggered the onset of LAD, which involves anti-basement membrane IgA antibody. Because the onset of KD was earlier than the appearance of HSV infection, we considered that KD and HSV were independent events. LAD did not relapse upon the resurgence of KD. Our hypothesis is that in this patient, LAD was triggered by two components, KD and HSV infection. We believe that this is a unique and interesting case to consider the etiology of LAD.

ACKNOWLEDGEMENTS

We are grateful to Mr. Katsumi Mizuta, Department of Microbiology, Yamagata Prefectural Institute of Public Health for the genetic analyses and Dr. Norito Ishii and Dr. Takashi Hashimoto, Department of Dermatology, Kurume University for the serum immunoblotting analysis.

Masahiro HAYASHI,[1,2] Fumiko MONMA,[1]
Yoshiyuki KATAGIRI,[1] Masakazu KAWAGUCHI,[1]
Tamio SUZUKI[1]

[1]*Department of Dermatology, Yamagata University School of Medicine, Yamagata, and* [2]*Division of Dermatology, Yamagata Prefectural Shinjo Hospital, Shinjo, Japan*

REFERENCES

1 Chorzelski TP, Jablonska S. IgA linear dermatosis of childhood (chronic bullous disease of childhood). *Br J Dermatol* 1979; **101**: 535–542.
2 Thune P, Eeg-Larsen T, Nilsen R. Acute linear IgA dermatosis in a child following varicella. *Arch Dermatol* 1984; **120**: 1237–1238.
3 Avci O, Okmen M, Cetiner S. Acetaminophen-induced linear IgA bullous dermatosis. *J Am Acad Dermatol* 2003; **48**: 299–301.
4 Kawasaki T. Acute febrile mucocutaneous syndrome with lymphoid involvement with specific desquamation of the fingers and toes in children. (In Japanese) *Jpn J Allerg* 1967; **16**: 178–222.
5 Shulman ST, Rowley AH. Advances in Kawasaki disease. *Eur J Pediatr* 2004; **163**: 285–291.
6 Rowley AH, Eckerley CA, Jäck HM, Shulman ST, Baker SC. IgA plasma cells in vascular tissue of patients with Kawasaki syndrome. *J Immunol* 1997; **159**: 5946–5955.
7 Rowley AH, Shulman ST, Mask CA *et al.* IgA plasma cell infiltration of proximal respiratory tract, pancreas, kidney, and coronary artery in acute Kawasaki disease. *J Infect Dis* 2000; **182**: 1183–1191.
8 Aurelius E, Johansson B, Sköldenberg B, Staland A, Forsgren M. Rapid diagnosis of herpes simplex encephalitis by nested polymerase chain reaction assay of cerebrospinal fluid. *Lancet* 1991; **337**: 189–192.
9 Kimura T, Miyazawa H, Watanabe K, Moriya T. Small pustules in Kawasaki disease. A clinicopathological study of four patients. *Am J Dermatopathol* 1988; **10**: 218–223.
10 Kwan YW, Leung CW. Pustulo-vesicular skin eruption in a child with probable Kawasaki disease. *Eur J Pediatr* 2005; **164**: 770–771.
11 Rowley AH, Shulman ST, Garcia FL *et al.* Cloning the arterial IgA antibody response during acute Kawasaki disease. *J Immunol* 2005; **175**: 8386–8391.
12 Rowley AH, Shulman ST, Spike BT, Mask CA, Baker SC. Oligoclonal IgA response in the vascular wall in acute Kawasaki disease. *J Immunol* 2001; **166**: 1334–1343.
13 Gupta M, Johann-Liang R, Bussel JB, Gersony WM, Lehman TJ. Elevated IgA and IgM anticardiolipin antibodies in acute Kawasaki disease. *Cardiology* 2002; **97**: 180–182.
14 Takeshita S, Kawase H, Shimizu T, Yoshida M, Sekine I. Increased production of serum IgA-class antibody to lipid A in Kawasaki disease. *Pediatr Int* 2002; **44**: 5–11.

Arch Dermatol Res (2010) 302:481–482
DOI 10.1007/s00403-010-1036-5

LETTER TO THE EDITOR

A missense mutation c.G2747A (p.R916Q) of *ADAR1* gene in dyschromatosis symmetrica hereditaria is not a novel mutation

Masahiro Hayashi · Tamio Suzuki

Received: 26 January 2010 / Accepted: 29 January 2010 / Published online: 19 February 2010

Dear Editor,

Dyschromatosis symmetrica hereditaria (DSH: OMIM no. 127400) is a rare pigmentary genodermatosis predominantly seen in Asia, including Japan, Taiwan and China. It is inherited in autosomal dominant manner and has high penetrance. Its clinical manifestations are intermingled hypo- and hyperpigmented macules on the dorsal aspects of hands, feet and the face, and they appear in infancy or early childhood [3].

We have shown that adenosine deaminase acting on RNA1 (*ADAR1*), also known as the double-stranded RNA-specific adenosine deaminase (*DSRAD*), is the responsible gene for DSH [1] and around 90 of various mutations have been reported. We have been making the database of *ADAR1* gene mutations reported to date. Figure 1 shows the schematic mutations.

We have read an article described by Xu et al. [4] that they reported two "novel" mutations of *ADAR1*, c.G2747A leading to p.R916Q in exon 9 and c.C3124T leading to p.R1042C in exon 12, respectively. The latter c.C3124T (p.R1042C) is certainly a novel mutation; however, former mutation c.G2747A (p.R916Q) has already been reported by our group [2].

We would be very grateful if the editor will check them and let the author correct the statement. We really appreciate your kindly cooperation.

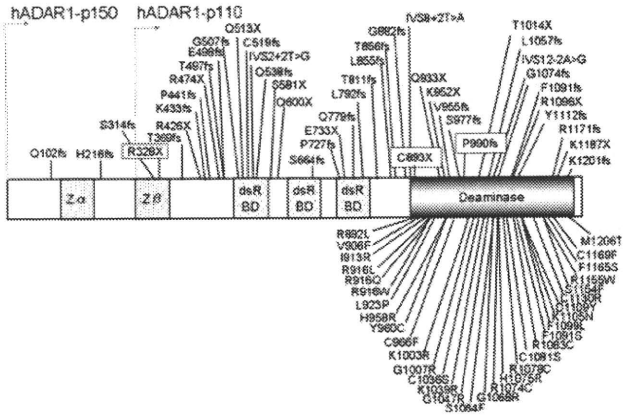

Fig. 1 Mutations of the *ADAR1* gene reported in patients with DSH. Mutations above the *horizontal axis* are nonsense, frameshift and splicing mutations and those *below* are missense mutations; *zα and zβ* Z-DNA-binding domains, *dsRBD* double-stranded RNA-binding domains, *deaminase* deaminase domain

Although many mutations of *ADAR1* have been detected, the pathogenesis and mechanism of onset of DSH have not been elucidated yet. Further investigations are needed to clarify them.

Conflict of interest statement The authors declare that they have no conflict of interest.

References

1. Miyamura Y, Suzuki T, Kono M, Inagaki K, Ito S, Suzuki N, Tomita Y (2003) Mutations of the RNA-specific adenosine deaminase gene (*DSRAD*) are involved in dyschromatosis symmetrica hereditaria. Am J Hum Genet 73:693–699
2. Suzuki N, Suzuki T, Inagaki K, Ito S, Kono M, Horikawa T, Fujiwara S, Ishiko A, Matsunaga K, Aoyama Y, Tosaki-Ichikawa H,

M. Hayashi (✉) · T. Suzuki
Department of Dermatology,
Yamagata University School of Medicine,
Iida-Nishi 2-2-2, Yamagata 990-9585, Japan
e-mail: CZK11223@nifty.ne.jp

Tomita Y (2007) Ten novel mutations of the *ADAR1* gene in Japanese patients with dyschromatosis symmetrica hereditaria. J Invest Dermatol 127:309–311
3. Tomita Y, Suzuki T (2004) Genetics of pigmentary disorders. Am J Med Genet C Semin Med Genet 131C:75–81
4. Xu Q, Xiao S, Huo J, Dong Y, Ren J, Wang X, Ma J, An J, Liu Y (2010) Identification of two novel *DSRAD* mutations in two Chinese families with dyschromatosis symmetrica hereditaria. Arch Dermatol Res. doi:10.1007/s00403-009-1027-6

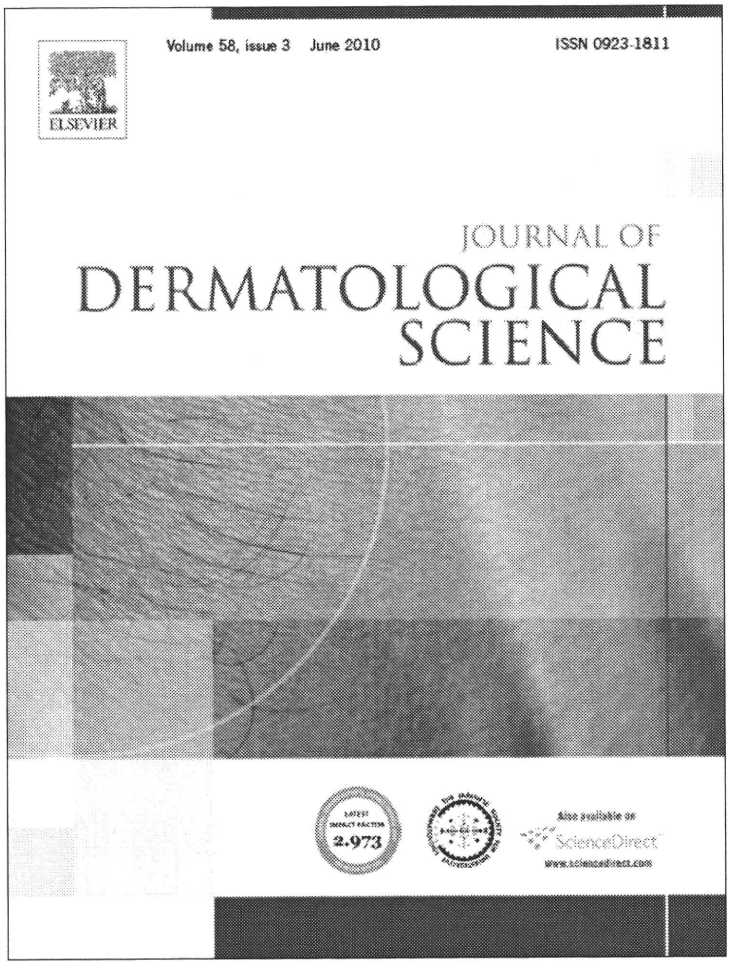

reported in another unrelated family too [6]. Whether are these two mutations hotspots that needs to be further validated.

To date, more than 90 different mutations have been reported. Clinical manifestations observed in the patients of all study, showed no obvious phenotypic variations and no evident genotype–phenotype correlations between affected individuals. We hope more findings of novel mutations would helpful for revealing the mechanism leading to DSH and further clarifying the relation between genotype and phenotype.

In conclusion, our results provide a significant addition to the DSH mutation database and will contribute further to the understanding of DSH genotype/phenotype correlations and to the pathogenesis of this disease.

Acknowledgments

We are grateful to the patients, their families and volunteers for providing blood samples. This work was supported by grants 30800991 and 200806981034 from the National Natural Science Foundation of China and the New Teacher Foundation of Doctor Spot Foundation.

References

[1] Toyama I. Dyschromatosis symmetrica hereditaria (in Japanese). Jpn J Dermatol 1929;27:95–6.
[2] Oyama M, Shimizu H, Ohata Y, et al. Dschromatosis symmetrica hereditaria: report of a Japanese family with the condition and a literature review of 185 cases. Br J Dermatol 1999;140:491–6.
[3] Zhang XJ, Gao M, Li M, et al. Identification of a locus for dyschromatosis symmetrica hereditaria at chromosome 1q11–1q21. J Invest Dermatol 2003;120:776–80.
[4] Miyamura Y, Suzuki T, Kono M, et al. Mutations of the RNA Specific Adenosine Deaminase Gene (DSRAD) are involved in dyschromatosis symmetrica hereditaria. Am J Hum Genet 2003;73:693–9.
[5] Bass BL, Weintraub H. An unwinding activity that covalently modifies its double-stranded RNA substrate. Cell 1988;55:1089–98.
[6] Sun XK, Xu AE, Chen JF, et al. The double-RNA-specific adenosine deaminase (DSRAD) gene in dyschromatosis symmetrica hereditaria patients: two novel mutations and one previously described [J]. Br J Dermatol 2005;153:342–5.
[7] Zhang XJ, He PP, Li M, et al. Seven novel mutations of the ADAR gene in Chinese families and sporadic patients with dyschromatosis symmetrica hereditaria (DSH). Hum Mutat 2004;23:629–30.
[8] Hou Y, Chen J, Gao M, et al. Five novel mutations of RNA specific adenosine deaminase gene with dyschromatosis symmetrica hereditaria. Acta Derm Venereol 2007;87:18–21.
[9] Furen Z, Hong L, Deke J, et al. Six novel mutations of the ADAR1 gene in Chinese patients with dyschromatosis symmetrica hereditaria. J Dermatol Sci 2008;50:109–14.
[10] Cho DS, Yang W, Lee JT, et al. Requirement of dimerization for RNA editing activity of adenosine deaminase acting on RNA. J Biol Chem 2003;278:17093–102.

Xiao-peng Wang
Wan-juan Wang
Jun-min Wang
Yan Liu*
Sheng-xiang Xiao*
Department of Dermatology, the Second Hospital, Xi'an Jiaotong University, 157 Xiwu Road, Xi'an, Shaanxi 710004, PR China

*Corresponding authors. Tel.: +86 13891928884; fax: +86 13709149292

E-mail addresses: yanliu95@163.com (Y. Liu)
Xiao_SX@163.com (S.-x. Xiao)

14 January 2010

doi:10.1016/j.jdermsci.2010.03.021

Letter to the Editor

Mutation analyses of patients with dyschromatosis symmetrica hereditaria: Five novel mutations of the *ADAR1* gene

Dyschromatosis symmetrica hereditaria (DSH: MIM#127400) shows an autosomal dominant pattern of inheritance with high penetrance, which is characterized by hyperpigmented and hypopigmented macules on the face and dorsal aspects of the extremities. The phenotypes appear in infancy or early childhood [1]. In Asia, the condition occurs predominantly among Japanese and Chinese individuals. Miyamura et al. have clarified that a heterozygous mutation of the adenosine deaminase acting on RNA 1 (*ADAR1*, formerly *DSRAD*) gene causes DSH in 4 Japanese DSH families [2]. Subsequently, more than 90 mutations have been reported from East Asian countries so far [3,4,5], which confirmed that the *ADAR1* gene is responsible for DSH not only in Japanese but also in other ethnic groups.

ADAR1 protein catalyzes the deamination of adenosine to inosine in double-stranded RNA substrates [6,7], which results in the creation of alternative splicing sites or alternations of the codon and thus leads to functional changes in the protein. The *ADAR1* gene is expressed ubiquitously, but the target RNA(s) in the skin still remain unknown. Although it has been reported that DSH may be caused by *ADAR1* haploinsufficiency [8,9], further molecular pathogenesis of DSH has not been clarified yet.

In this study, we describe mutation analyses of a Chinese and 9 Japanese families with DSH. We detected 5 novel and 4 known mutations, and failed to find any mutation in 1 Japanese family. Five novel mutations included 3 missense mutations (c.T2878A, p.Y960N; c.A3116C,p.K1039T; c.A3182G,p.Y1061C), 1 nonsense mutation (c.C1190A,p.S397X), and 1 two-nucleotide deletion mutation (c.1096-1097delAA,p.K366fs) in 1 family and 4 sporadic patients (Table 1). The mutational analysis of the *ADAR1* gene was performed as previously described [10]. Three novel missense mutations that altered amino acids conserved among all known species, including pufferfish, zebrafish, frog, rat, mouse, cow, and human within the deaminase domain of ADAR1 protein. These mutations were not detected in the control blood samples of the surveyed 100 unrelated, normally pigmented Japanese adults. Therefore, we consider these mutations pathologic with no functional activity. The patients originally consulted us for their skin conditions. All patients phenotypically presented typical macules on the dorsal aspects of the hands, feet, lower arms and lower legs, and freckle-like macules on the face. Informed consent and blood samples of patients were obtained under protocols approved by the Ethics Committee of Yamagata University School of Medicine.

The missense mutations at codon 960, tyrosine to cysteine and codon 1039, lysine to arginine have been already reported [5]. Here, we also reported same codon changes not to same amino acids but to asparagine (patient no. 2) and threonine (patient no. 1), respectively. So far, all known missense mutations are located within the deaminase domain [5], which encompasses amino acids 886–1221, suggesting that this domain is critical for enzyme

Table 1
Novel mutations of the *ADAR1* gene.

Patient no.	Patient's pedigree			Mutation			Onset year-old	Polymorphism	Novel or known
	Incidence	Affected individuals	Unaffected individuals	Nucleotide change[a]	Amino-acid change	Position			
1	Sporadic	1	–	c.A3116C	p.K1039T	Exon 12	3	c.A1151G, p.K384R in Exon 2, IVS4-20C>T, c.G2682A, p.V894V in Exon 9, IVS14+8A>G	Novel
2	Sporadic	1	–	c.T2878A	p.Y960N	Exon 10	1	c.G2682A, p.V894V in Exon 9	Novel
3	Familial	3	2	c.C3286T	p.R1096X	Exon 13	2	c.A1151G, p.K384R in Exon 2, c.G2682A, p.V894V in Exon 9 IVS14+8A>G	Known
4	Sporadic	1	–	c.1096-1097delAA	p.p.K366fs	Exon 2	1	c.G2682A, p.V894V in Exon 9	Novel
5	Familial	4	3	c.C1190A	p.S397X	Exon 2	3	IVS14+8A>G	Novel
6	Familial	2	1	c.C2746T	p.R916W	Exon 9	2	c.A1151G, p.K384R in Exon 2, IVS14+8A>G	Known
7[b]	Familial	3	6	c.C3247T	p.R1083C	Exon 13	6	None	Known
8	Sporadic	1	–	c.3169delC	p.L1057fs	Exon 12	3	c.G2682A, p.V894V in Exon 9, IVS14+8A>G	Known
9	Sporadic	1	–	c.A3182G	p.Y1061C	Exon 12	3	c.A1151G, p.K384R in Exon 2, c.G2682A, p.V894V in Exon 9, IVS14+8A>G	Novel
10	Familial	3	2	No mutation	–	–	2	c.A1151G, p.K384R in Exon 2, c.G2682A, p.V894V in Exon 9,	–

[a] GenBank accession no. NM_001111.3. Position 1 is A of the translation initiation codon.
[b] Chinese family.

function. The result in this study suggests that these codons might be hot spot for mutation within the deaminase domain.

The family of no. 10 revealed the typical phenotypes of DSH, hyperpigmented and hypopigmented macules on the face and dorsal aspects of the extremities, as shown in Fig. 1A–C. However, we could find any pathological mutation neither in SSCP nor sequencing of all exons and flanking regions. Furthermore, we examined *ADAR1* gene expression in peripheral blood cells from the affected individuals of no.10 family using RQ-PCR method [9], and then, confirmed that an amount of the expression was similar to that of a healthy control (Fig. 1D), indicating that there might be no mutation in the promoter region of *ADAR1* gene. These results might suggest locus heterogeneity for the disease. We planned to obtain experimental evidence for the possibility with tests for genetic linkage analysis of the family of patient 10. However, we could not test it, because DNA only from the affected, not the unaffected could be available. So far, there has been no report on the ADAR1 enzymatic activity in blood or skin tissue of the patient with DSH. If a convenient assay system for the ADAR1 protein using the patient's sample is established and available to us, we suppose that the enzymatic activity of patient no. 10 may be similar to those of healthy controls, on the other hand those of other patients in whom we could detect mutations of the *ADAR1* gene may decrease by one half, demonstrating the possibility for the locus heterogeneity.

In conclusion, we have found 5 novel mutations in the *ADAR1* gene of 1 DSH pedigree and 4 sporadic individuals, 4 recurrent mutations in 3 pedigrees and 1 sporadic individuals, and no mutation in a pedigree with typical phenotypes of DSH. These results may provide new insight into the pathogenesis of DSH.

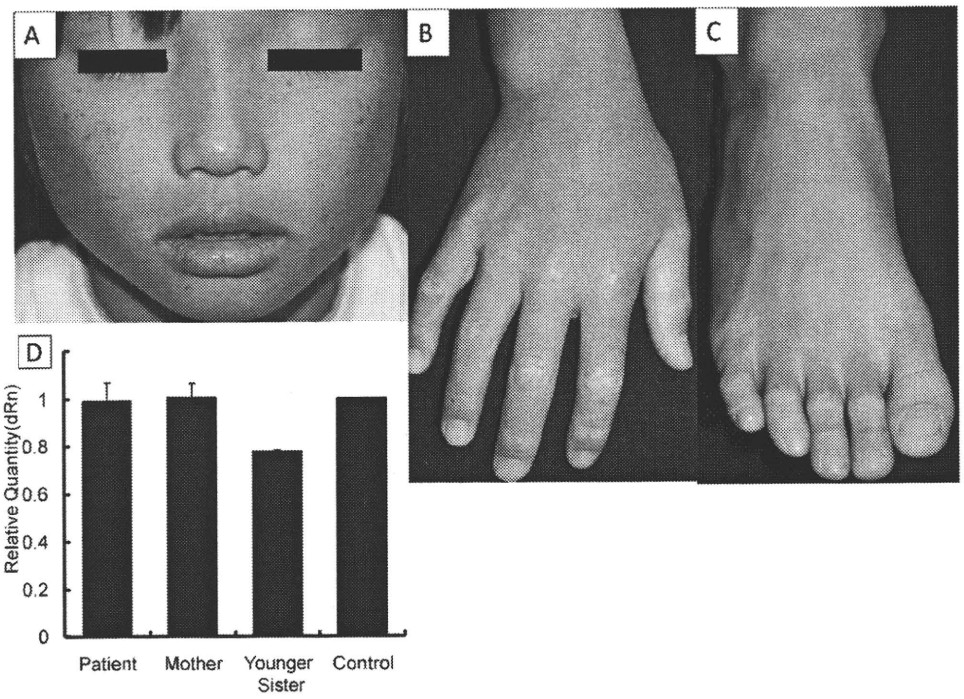

Fig. 1. Clinical phenotypes of patient no. 10 with freckle-like macules on the face (A) and a mixture of hyperpigmented and hypopigmented macules distributed on the back of her hand (B) and the top of her feet (C). Relative quantity of *ADAR1* transcripts of the affected individuals of family no. 10 (D). Data derived from real-time quantitative RT-PCR is expressed as mean ± S.D. of 3 independent experiments performed in triplicate. Mother and the younger sister of the patient no.10 family were affected.

Electronic database information

Accession numbers and URLs for data in this paper are as follows: GenBank, http://www.ncbi.nlm.nih.gov/Genbank/ (for the cDNA of human *ADAR1* [accession number NM_001111.3]).

Acknowledgments

We are grateful to the patients, their families and volunteers for providing blood samples. This work was supported by a grant from Ministry of Health, Labor, and Welfare of Japan (Health and Labor Sciences Research Grants; Research on intractable diseases; H21-181).

References

[1] Tomita Y, Suzuki T. Genetics of pigmentary disorders. Am J Med Genet C Semin Med Genet 2004;131C:75–81.
[2] Miyamura Y, Suzuki T, Kono M, Inagaki K, Ito S, Suzuki N, et al. Mutations of the RNA-specific adenosine deaminase gene (*DSRAD*) are involved in dyschromatosis symmetrica hereditaria. Am J Hum Genet 2003;73:693–9.
[3] Zhang F, Liu H, Jiang D, Tian H, Wang C, Yu L. Six novel mutations of the *ADAR1* gene in Chinese patients with dyschromatosis symmetrica hereditaria. J Dermatol Sci 2008;50:109–14.
[4] Kondo T, Suzuki T, Mitsuhashi Y, Ito S, Kono M, Komine M, et al. Six novel mutations of the *ADAR1* gene in patients with dyschromatosis symmetrica hereditaria: Histological observation and comparison of genotypes and clinical phenotypes. J Dermatol 2008;35:395–406.
[5] Hayashi M, Suzuki T. A missense mutation c.G2747A (p.R916Q) of ADAR1 gene in dyschromatosis symmetrica hereditaria is not a novel mutation. Arch Dermatol Res 2010. doi: 10.1007/s00403-010r-r1036-5.
[6] Bass BL, Weintraub H. An unwinding activity that covalently modifies its double-stranded RNA substrate. Cell 1988;55:1089–98.
[7] Wagner RW, Smith JE, Cooperman BS, Nishikura KA. Double-stranded RNA unwinding activity introduces structural alterations by means of adenosine to inosine conversions in mammalian cells and *Xenopus* eggs. Proc Natl Acad Sci USA 1989;86:2647–51.
[8] Liu Q, Jiang L, Liu WL, Kang XJ, Ao Y, Sun M, et al. Two novel mutations and evidence for haploinsufficiency of the *ADAR* gene in dyschromatosis symmetrica hereditaria. Br J Dermatol 2006;154:636–42.
[9] Murata I, HozumiY, Kawaguchi M, Katagiri Y, Yasumoto S, Kubo Y, et al. Four Novel Mutations of the *ADAR1* Gene in dyschromatosis symmetrica hereditaria. J Dermatol Sci 2009;53:76–7.
[10] Suzuki N, Suzuki T, Inagaki K, Ito S, Kono M, Fukai K, et al. Mutation analysis of the *ADAR1* gene in dyschromatosis symmetrica hereditaria and genetic differentiation from both dyschromatosis universalis hereditaria and acropigmentatio reticularis. J Invest Dermatol 2005;124:1186–92.

Ichidai Murata
Masahiro Hayashi
Yutaka Hozumi
Department of Dermatology, Yamagata University School of Medicine, Yamagata, Japan

Kazuyasu Fujii
Department of Dermatology, Okayama University Graduate School of Medicine and Dentistry, Okayama, Japan

Yoshihiko Mitsuhashi
Department of Dermatology, Tokyo Medical University, Tokyo, Japan

Naoki Oiso
Department of Dermatology, Kinki University School of Medicine, Osaka-Sayama, Japan

Kazuyoshi Fukai
Department of Dermatology, Osaka City University Graduate School of Medicine, Osaka, Japan

Nozomi Kuroki
Department of Dermatology, Chigasaki Municipal Hospital, Chigasaki, Japan

Yasuki Mori
Department of Dermatology, Iwate Prefectural Central Hospital, Morioka, Japan

Atsushi Utani
Department of Dermatology, Kyoto University Graduate School of Medicine, Kyoto, Japan

Yasushi Tomita
Department of Dermatology, Nagoya University Graduate School of Medicine, Nagoya, Japan

Yasuyuki Fujita
Department of Dermatology, Hokkaido University Graduate School of Medicine, Sapporo, Japan

Tamio Suzuki*
Department of Dermatology, Yamagata University School of Medicine, Yamagata, Japan

*Corresponding author at: Department of Dermatology, Yamagata University Faculty of Medicine, 2-2-2, Iida-Nishi, Yamagata 990-9585, Japan.
Tel.: +81 23 628 5359/5361; fax: +81 23 628 5364

E-mail address: tamsuz@med.id.yamagata-u.ac.jp (T. Suzuki)

16 March 2010

doi:10.1016/j.jdermsci.2010.04.001

Letter to the Editor

Schöpf-Schulz-Passarge syndrome resulting from a homozygous nonsense mutation in *WNT10A*

Schöpf-Schulz-Passarge syndrome (SSPS; OMIM 224750) is an autosomal recessive inherited form of ectodermal dysplasia characterized by eyelid cysts (apocrine hidrocystomas), palmoplantar keratoderma, hypodontia, hyperhidrosis, hypotrichosis and onychodystrophy, as well as other, often variable, ectodermal developmental anomalies [1,2]. SSPS shows clinical overlap with odonto-onycho-dermal dysplasia (OODD; OMIM 277980), but the eyelid cysts are a typical feature of SSPS [1].

In 2007, the molecular pathology of OODD was shown to involve a loss-of-function mutation in the *WNT10A* gene, which encodes the wingless-type MMTV integration site family member 10A [3], and a further pathogenic mutation in *WNT10A* was subsequently shown in another family with OODD [4]. In 2009 and 2010, additional nonsense and missense mutations in *WNT10A* were delineated, not only in OODD, but also in individuals with severe oligodontia and various other manifestations of ectodermal dysplasia, including a family with SSPS [5]. To date, five nonsense mutations (p.Trp9X, p.Cys107X, p.Arg128X, p.Glu233X, and p.Cys376X) and three missense mutations (p.Arg128Gln, p.Ala131-

11112 J. Agric. Food Chem. 2010, 58, 11112–11118
DOI:10.1021/jf102650d

JOURNAL OF AGRICULTURAL AND FOOD CHEMISTRY
ARTICLE

Extract of Passion Fruit (*Passiflora edulis*) Seed Containing High Amounts of Piceatannol Inhibits Melanogenesis and Promotes Collagen Synthesis

YUKO MATSUI,*,† KENKICHI SUGIYAMA,† MASANORI KAMEI,† TOSHIO TAKAHASHI,† TAMIO SUZUKI,‡ YOHTARO KATAGATA,§ AND TATSUHIKO ITO||

†Research Institute, Morinaga and Company, Limited, 2-1-1 Shimosueyoshi, Tsurumi-ku, Yokohama 230-8504, Japan, ‡Department of Dermatology, Yamagata University School of Medicine, Yamagata University, 2-2-2 Iidanishi, Yamagata 990-9585, Japan, §Faculty of Agriculture and Life Science, Hirosaki University, 3 Bunkyo-cho, Hirosaki 036-8561, Japan, and ||Health Care Division, Morinaga and Company, Limited, 2-1-1 Shimosueyoshi, Tsurumi-ku, Yokohama 230-8504, Japan

The effect of passion fruit, the fruit of *Passiflora edulis*, on melanin inhibition and collagen synthesis was studied using cultured human melanoma and fibroblast cells. Passion fruit was divided into three parts, rind (PF-R), pulp (PF-P), and seed (PF-S), and each part was extracted using 80% ethanol. The concentration of polyphenols was higher in PF-S than in PF-R or PF-P. Treatment of melanoma cells with PF-S led to inhibition of melanogenesis. In addition, the production of total soluble collagen was elevated in dermal fibroblast cells cultured in the presence of PF-S. PF-R and PF-P did not yield these effects. Furthermore, the removal of polyphenols from PF-S led to the abolishment of the effects described above. We discovered that piceatannol (3,4,3′,5′-tetrahydroxy-*trans*-stilbene) is present in passion fruit seeds in large amounts and that this compound is the major component responsible for the PF-S effects observed on melanogenesis and collagen synthesis.

KEYWORDS: *Passiflora edulis*; piceatannol; passion fruit seed; melanin; collagen

INTRODUCTION

Tropical fruits and vegetables are beneficial for human health. Passifloraceae is a well-known tropical plant from the South American tropical forests, and its leaves, vines, and flowers are used as medicinal herbs. There are many reports on the actions of Passifloraceae herbs, which include its anti-anxiety effect in humans (*1*) and its anti-inflammatory and cough-suppressant effects in mice (*2*, *3*). However, studies on the fruit of *Passiflora edulis* from the Passifloraceae family, which is known as passion fruit, are limited.

Passion fruit is usually eaten in its natural state, with the seeds, or processed as tropical juice. Passion fruit contains many phytochemicals, such as polyphenolic compounds (*4*) and carotenoid families (*5*), and vitamin C (*6*), which are known as being beneficial for the skin. The health effects of the polyphenols contained in many natural plants, including tropical fruits, have been increasingly and energetically studied. The content of polyphenols in various tropical fruits (*7*), as well as the bioactive effects of tropical fruits, such as acai and mangosteen (*8*, *9*), have been reported.

Skin abnormalities, such as aging, are caused by genetic and environmental factors. In addition, the damage to skin by UV exposure, mental and environmental stress, eating habits, etc., leads to skin pigmentation, wrinkles, and even skin cancer. Melanin is the pigment that colors the skin. Although melanin is important for protection from UV rays, production to an excessive degree leads to skin erythema, freckles, and other skin disorders. Many bioactive substances from naturally occurring plants are studied for the prevention of melanogenesis. In those reports, the effect of polyphenols from safflower seed, grape seed (*10*, *11*), and many other edible plants are described. Collagen, which is another molecule that is essential for skin health, plays many important roles in the body, including cell−cell adhesion, cell proliferation, and cell differentiation. The functional properties of the skin considerably depend upon the quantity and condition of the collagen present in the dermis. Some foods and food components contribute to the maintenance of the collagen condition in the skin or inhibit collagen-degrading factors, e.g., royal jelly (*12*) and polyphenols, such as catechin and flavonoids (*13*, *14*). To prevent skin damage and maintain its protective potency against environmental agents, there is an increased research focus on compounds that target the skin. As described above, polyphenols play important roles in dermal cells; thus, we predicted the effectiveness of passion fruit in the promotion and maintenance of skin health.

The aim of this paper was to investigate the effect of passion fruit on melanogenesis and collagen synthesis in dermal cells and identify the component responsible for these effects.

MATERIALS AND METHODS

Materials. Piceatannol (3,4,3′,5′-tetrahydroxy-*trans*-stilbene), resveratrol (3,5,4′-trihydroxy-*trans*-stilbene), and polyvinylpolypyrrolidone

*To whom correspondence should be addressed: Research Institute, Morinaga and Co., Ltd., 2-1-1 Shimosueyoshi, Tsurumi-ku, Yokohama 230-8504, Japan. Telephone: +81-45-571-2504. Fax: +81-45-571-6109. E-mail: y-matsui-jd@morinaga.co.jp.

 Published on Web 09/07/2010

(PVPP) were purchased from Sigma-Aldrich Japan (Tokyo, Japan). Culture reagents, such as Dulbecco's modified Eagle's medium (DMEM), Medium 106S, phosphate-buffered saline (PBS), low-serum growth supplement (LSGS), glutamine, penicillin, streptomycin, gentamicin, amphotericin B, and trypsin−ethylenediaminetetraacetic acid (EDTA), were purchased from Invitrogen (Carlsbad, CA), and fetal bovine serum (FBS) was purchased from Biowest (Maine-et-Loire, France). Synthetic melanin was purchased from Nacalai Tesque (Kyoto, Japan), and the Sircol soluble collagen assay kit was purchased from Biocolor Life Science Assays (Newtownabbey, U.K.). Other reagents were purchased from Wako Pure Chemicals (Tokyo, Japan).

Sample Preparation. Commercial whole passion fruit (product of Kagoshima, Japan) was divided into three parts: rind, pulp, and seed. Each part was freeze-dried, milled, and extracted twice using 10-fold amounts of 80% (v/v) ethanol, by shaking at room temperature. The extract solution was centrifuged at 3000*g* for 10 min to obtain the supernatant, which was filtered through a paper filter to remove the sediment. Aliquots containing the extracts were evaporated, freeze-dried, and dissolved in distilled water at the concentration of 100 mg/mL (for rind and pulp) or 20 mg/mL (for seeds). The extract solutions were filtered using a hydrophilic membrane filter (Kanto Kagaku, Japan), with a pore size of 0.45 μm. The rind, pulp, and seed of passion fruit extracts were termed PF-R, PF-P, and PF-S, respectively.

Polyphenol Quantification. The polyphenol concentration was measured according to a modified Folin−Ciocalteu method, as described previously (*15*), using (−)-epicatechin to obtain the standard curve for polyphenol. To examine whether polyphenols contribute to the inhibition of melanogenesis and collagen synthesis, polyphenols were removed from PF-S via absorption with PVPP because the amide bonds of PVPP form hydrogen bonds with the hydroxyl groups of polyphenols. PVPP was swollen in distilled water, added to 20 mg/mL PF-S, and stirred for 30 min. The solution was centrifuged at 12000*g* for 15 min to obtain PVPP-treated PF-S. The polyphenol concentration was measured again using the Folin−Ciocalteu method, to confirm that the polyphenols were removed. The experiment was carried out in triplicate.

Fractionation of PF-S. High-performance liquid chromatography (HPLC) analysis was carried out using a Shimadzu system controller SCL-10A, a UV detector RF-10A, and a fraction collector FRC-10A (Shimadzu, Kyoto, Japan). Samples were fractionated via reverse-phase HPLC using an octa decyl silyl (ODS) column (Mightysil RP-18 GP250-10, 250 × 10 mm inner diameter, 5 μm, Kanto Kagaku, Tokyo, Japan). A total of 4 mL of 20 mg/mL PF-S was injected into the HPLC apparatus using a linear gradient of 0−30% at 0−10 min from solvent B to solvent A, where solvent A consisted of a water/acetonitrile/acetic acid (400:10:1, v/v/v) mix and solvent B consisted of a solvent A/methanol (2:1, v/v) mix. The temperature of the column was maintained at 40 °C. Measurements were carried out at a flow rate of 3 mL/min, and the wavelength used for UV detection was 280 nm. The absorbance of each fraction was measured with a spectrophotometer (V-630, JASCO Corporation, Tokyo, Japan). The HPLC chromatogram was divided into three fractions. Fraction 1 (tubes 1−17; 0−30 min), fraction 2 (tubes 18−23; 31−40 min), and fraction 3 (tubes 23−39; 41−70 min). The solvents used for HPLC were eliminated from each fraction by evaporation and freeze-drying, and the remaining extracts were dissolved in distilled water to maintain a concentration of 100 μg/mL. Each fraction and 100 μg/mL of PF-S served as samples for the measurement of melanin and soluble collagen, as described below.

Qualitative Analysis and Determination of Piceatannol. Ground passion fruit seeds were extracted with 70% (v/v) acetone 3 times, with shaking at room temperature. Samples were evaporated and freeze-dried to obtain crude extracts. A total of 100 mg of crude extract was suspended in 50 mL of 50% methanol solution and centrifuged at 1500*g* for 5 min. This supernatant was separated via reverse-phase liquid chromatography using a linear-gradient mode, as follows. Chromatographic measurements were carried out using an Agilent 1100 series liquid chromatography/mass spectrometry (LC/MS) system (Agilent Technologies, Tokyo, Japan) that included a photodiode array (PDA) detector. The HPLC column used in this study was Inertsil ODS-3 (150 × 2.1 mm inner diameter, 5 μm, GL Science, Tokyo, Japan). The mobile phase consisted of (A) water and (B) acetonitrile (v/v) using an initial gradient elution of 10% B and a gradient of 10−45% B at 0−25 min. The column temperature was maintained at 45 °C. All measurements were carried out at a flow rate of 0.25 mL/min using a detector wavelength of 280 nm. The mass spectrometric data were collected in full-scan mode, from m/z 200 to 1000.

Cells and Cell Culture. Melanin-producing MNT-1 human melanoma cells (a gift from Dr. V. J. Hearing, Laboratory of Cell Biology, National Cancer Institute, National Institutes of Health, Bethesda, MD) were cultured in DMEM containing 10% FBS, 4 mM glutamine, 100 units/mL penicillin, and 100 μg/mL streptomycin.

SF-TY human dermal fibroblast cells (Health Science Research Resources Bank, Tokyo, Japan) were cultured in Medium 106S supplemented with 5% LSGS, 10 μg/mL gentamicin, and 0.25 μg/mL amphotericin B. Melanoma and fibroblast cells were incubated at 37 °C under 5% CO_2 and 95% air.

Measurement of Melanin Content. MNT-1 cells were seeded at a density of 7.0×10^4 cells/well in 12-well culture plates and were cultured for 24 h. Subsequently, the medium was replaced with fresh DMEM containing various concentrations of PF-R, PF-P, PF-S, and kojic acid [5-hydroxy-2-(hydroxymethyl)-4-pyrone], which was used as a positive control. After 72 h of culture, cells were washed with PBS and trypsinized with 0.25% trypsin containing 0.02% EDTA. The number of cells harvested was counted. To measure the melanin produced in these cells, harvested cells were washed twice with PBS and centrifuged at 300*g* for 5 min at 4 °C, to obtain cell pellets. The cell pellets were dissolved in 500 μL of 1 N NaOH and quantified for melanin content using spectrophotometry at a wavelength of 415 nm. The concentration of the melanin produced was calculated from the standard curves using synthetic melanin dissolved in 1 N NaOH. The melanin produced was expressed as a concentration ratio relative to control MNT-1 cells that were not treated with any of the extracts or kojic acid.

Measurement of Soluble Collagen Content. SF-TY cells were seeded at a density of 1.7×10^4 cells/well in 48-well culture plates and were cultured for 24 h. Subsequently, the medium was replaced with fresh medium containing various concentrations of PF-R, PF-P, PF-S, and ascorbate, which was used as a positive control. After 72 h of culture, the medium was collected and assayed for soluble collagen content using the Sircol soluble collagen assay kit, according to the instructions of the manufacturer. Briefly, supernatants of SF-TY cells were centrifuged at 12000*g* for 4 min, and 100 μL of each supernatant was mixed with 1 mL of Sircol dye and shaken for 30 min. The aliquot was then centrifuged at 12000*g* for 10 min to pellet the collagen−dye complex. After the suspension was decanted, droplets were dissolved in 0.75 mL of Sircol alkali reagent. The concentration of collagen was measured using spectrophotometry at a wavelength of 540 nm, using soluble collagen for the standard curve. The value of the blank (i.e., the medium alone) was subtracted from each sample, to remove the contribution of the collagen contained in FBS. Total soluble collagen was expressed as a concentration ratio relative to control SF-TY cells that were not treated with any of the extracts or ascorbate. Adherent cells were washed twice with PBS and harvested using trypsin, for cell counting.

Statistical Analyses. Data represent the mean ± standard deviation (SD) for the indicated number of experiments. Statistical significance of the difference between the corresponding control was carried out using the paired t test, where *, **, and *** represented $p < 0.1$, $p < 0.05$, and $p < 0.01$, respectively.

RESULTS

Total Polyphenol Content. Total polyphenol content in freeze-dried rind, pulp, and seed was measured using the Folin−Ciocalteu method. The results showed that PF-S contained a much larger amount of polyphenols compared to PF-R and PF-P, because polyphenols represented 33% of the freeze-dried seeds. The rind and pulp contained only 4 and 0.2% polyphenols, respectively. The part ratio occupying raw passion fruit was as follows: rind, 40%; pulp, 48%; and seed, 12%, and the freeze-drying process reduced the weight of each part by 14, 18, and 45%, respectively. This means that the calculated polyphenol content in the raw fruit was 0.22, 0.02, and 1.8%, respectively. Although the seed represents only 12% of the whole fruit, in weight, 88% of the total polyphenol content was found in the seed.

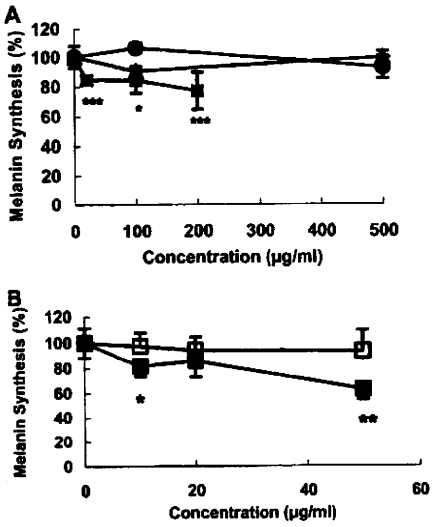

Figure 1. Comparison of melanin synthesis associated with (A) 80% ethanol extracts of passion fruit rind (PF-R; ●), pulp (PF-P; ▲), and seed (PF-S; ■). (B) PF-S (■) and PVPP-treated PF-S (□). Data are expressed as means ± SD (n = 4). Statistical analyses were performed using the paired t test: *, $p < 0.1$; **, $p < 0.05$; ***, $p < 0.01$.

Inhibition of Melanogenesis by PF-R, PF-P, and PF-S in Melanoma Cells. Melanin synthesis was measured in melanin-producing human melanoma cells. Cells were cultured in the presence or absence of passion fruit extracts, and the melanin produced was compared to that of control cells, which were cultured in the absence of extracts. None of the samples inhibit cell growth at the concentrations examined (data not shown). As shown in **Figure 1A**, a significant decrease in melanin synthesis was observed when PF-S was applied to the melanoma cell culture at 20 μg/mL. In contrast, PF-R and PF-P did not inhibit melanin synthesis, although the concentration of these extracts was higher than that of PF-S. Kojic acid, which was applied for positive control, showed statistical significance ($p < 0.05$) at 10 μg/mL. To examine whether the polyphenols contained in PF-S are effective in the prevention of melanogenesis, polyphenols were removed from PF-S via PVPP treatment. More than 95% of the polyphenols were removed. PF-S inhibited melanin synthesis significantly, while PVPP-treated PF-S did not lead to inhibition of melanin synthesis (**Figure 1B**).

Soluble Collagen Production in Dermal Fibroblast Cells after PF-R, PF-P, and PF-S Treatment. Total soluble collagen was quantified in the culture medium of human dermal fibroblast cells (**Figure 2A**). Cells were cultured in the presence or absence of passion fruit extracts, and the collagen produced was compared to that of control cells, which were cultured in the absence of extracts. None of the samples inhibit cell growth at the concentrations examined (data not shown). Soluble collagen synthesis increased in a dose-dependent manner after the addition of PF-S to the cell culture. Ascorbate, which was applied for positive control, showed statistical significance ($p < 0.1$) at 25 μg/mL. However, similar to what was observed in melanoma cells, PF-R and PF-P did not increase collagen synthesis. Furthermore, PF-S led to a significant increase in the soluble collagen concentration in the medium (at 100 μg/mL) (**Figure 2B**), whereas the removal of polyphenols from PF-S via PVPP treatment did not lead to an increase of soluble collagen content in the culture medium.

Fractionation of PF-S and Measurement of Melanin and Soluble Collagen Synthesis. To determine the component of PF-S that was responsible for the inhibition of melanogenesis and soluble collagen synthesis, PF-S was fractionated using HPLC.

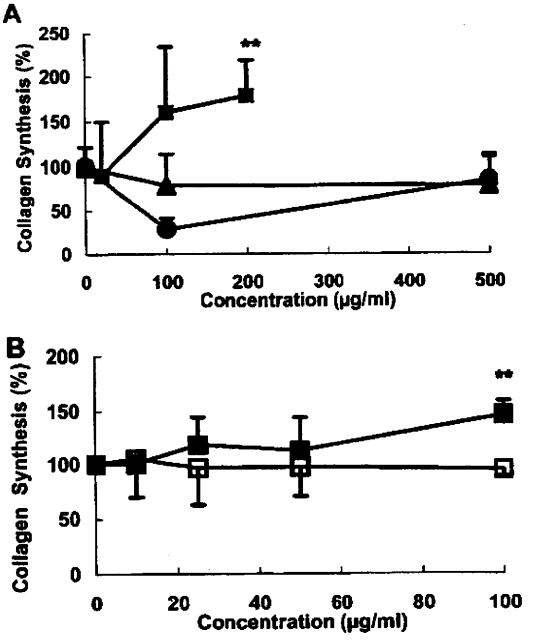

Figure 2. Soluble collagen synthesis associated with (A) 80% ethanol extracts of passion fruit rind (PF-R; ●), pulp (PF-P; ▲), and seed (PF-S; ■). (B) PF-S (■) and PVPP-treated PF-S (□). Data are expressed as means ± SD (n = 3). Statistical analyses were performed using the paired t test: *, $p < 0.1$; **, $p < 0.05$.

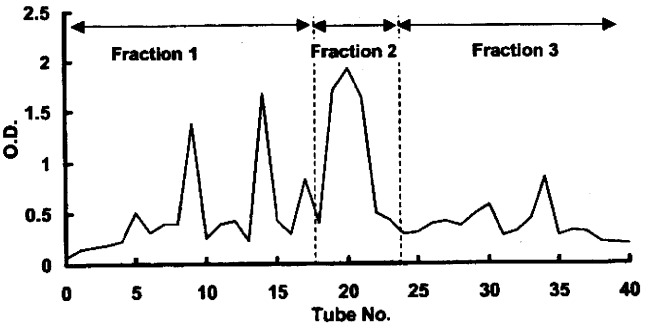

Figure 3. Absorbance of the fractioned 80% ethanol extracts of passion fruit seed (PF-S), obtained using reverse-phase chromatography with an ODS column. The three fractions were divided as fraction 1 (tubes 1−17; 0−18 min), fraction 2 (tubes 18−23; 19−22 min), and fraction 3 (tubes 23−39; 23−70 min).

Figure 3 shows the absorbance of each fraction of PF-S obtained by HPLC. One significant peak was observed at a retention time of ~20 min. PF-S was divided into three fractions, fractions 1−3, where fraction 2 contained the significant peak and fractions 1 and 3 were fractions with a retention time that was earlier and later, respectively, compared to fraction 2. The three fractions, with a concentration equivalent to 100 μg/mL, were added to MNT-1 and SF-TY cells to examine inhibition of melanogenesis and soluble collagen synthesis, as described previously. As shown in **Figure 4A**, fraction 2 inhibited melanin synthesis to a similar extent, as did PF-S (p = 0.103). Soluble collagen synthesis was also elevated in fraction-2-treated cells, which demonstrates that the components responsible for these effects are contained in fraction 2 (**Figure 4B**). However, only PF-S showed a significant increase in collagen synthesis.

Determination of Piceatannol. The polyphenol contained in passion fruit seed was determined by chromatographic measurements. The specific peak 1, as described in **Figure 5**, corresponded